Delayed-detection measurement of atomic Na $3p\ ^2P_{3/2}$ hyperfine structure using polarization quantum-beat spectroscopy

Wo Yei
Physics Department, Old Dominion University, Norfolk, Virginia 23529

A. Sieradzan
Physics Department, Central Michigan University, Mt. Pleasant, Michigan 48859

M. D. Havey
Physics Department, Old Dominion University, Norfolk, Virginia 23529

(Received 13 April 1993)

A subnatural linewidth measurement of magnetic-dipole and electric-quadrupole hyperfine coupling constants in the atomic Na $3p\ ^2P_{3/2}$ level are reported. The measurements are made using a pump–delayed-probe method, with delays ranging to 135 ns, more than eight times the natural lifetime of the $3p\ ^2P_{3/2}$ level. A measurement of hyperfine-induced beats in the time evolution of the electronic alignment permitted determination of the hyperfine frequencies to well beyond the natural width in that level. Hyperfine coupling constants $A=18.534(15)$ MHz and $B=2.724(30)$ MHz are obtained, these being more than 2 times more precise than any previous determination of those quantities.

PACS number(s): 35.10.Fk, 32.30.−r, 32.80.−t, 42.62.Fi

I. INTRODUCTION

Experiments done over the course of many decades have led to very precisely determined hyperfine structure in the ground state of numerous atoms [1]. Measurements of excited-state hyperfine structure have been much more limited, in part because of the difficulty of generating large populations in the states and because of the impeding effect of spontaneous decay of the levels on the attainable spectral resolution. A variety of laser-based approaches, coupled in some cases with subnatural linewidth techniques, have led to precisions for nonmetastable states of about 10^{-4} (in the coupling constants) for some cases [1–3]. Hyperfine measurements in excited electronic states with $j\neq 0$ give global information on higher multipoles of the nuclear charge and current distributions [4]. Precise measurements of excited-state properties such as hyperfine structure and oscillator strengths push the limits of excited-state wave-function calculations, for those quantities can depend significantly on core polarization and electron correlation effects [5,6]. Accurate wave functions are important in many applications, including the analysis of atomic parity-violation experiments [6].

Precision excited-state hyperfine measurements can also impact other areas of research. For example, two reports describing a discrepancy between nuclear-quadrupole moments Q, as obtained from muonic x-ray spectra and as derived from atomic hyperfine measurements, have recently appeared. Sundholm and Olsen [7] calculated electric-field gradients that were combined with atomic hyperfine measurements of quadrupole coupling constants B to obtain nuclear-quadrupole moments in ^{23}Na and ^{27}Al. They obtained values for $Q(^{23}\mathrm{Na})$ and $Q(^{27}\mathrm{Al})$ differing from muonic ones by $+8\%$ in the former case and by -7% in the latter. These discrepancies correspond to several quoted error intervals in either of the determinations. More recently, Möller *et al.* [8] have measured hyperfine structure in numerous electronic multiplets of isotopes of europium. In a comparison of the electric-quadrupole coupling constants for two Eu isotopes, they found $Q(^{151}\mathrm{Eu})/Q(^{153}\mathrm{Eu})=0.391\,84(22)$. This ratio as deduced from muonic x-ray spectra is 0.3744(53). The two ratios differ by more than 3 times the quoted error in the muonic x-ray measurements. This is a strong result, for electronic structure effects should have limited influence on the ratio obtained from atomic hyperfine measurements.

In this paper, a precise measurement of the hyperfine structure in the $3p\ ^2P_{3/2}$ level of ^{23}Na is reported; the measured magnetic-dipole (A) and electric-quadrupole (B) coupling constants in that level are determined with an accuracy more than 2 times higher than that previously obtained by Krist *et al.* [9]. In the following sections, the details of our experimental approach are presented. These are followed by the experimental results and discussion of the various systematic effects which may influence the determination of the hyperfine coupling constants. Comparison of our measurements with previous determinations of A and B in the atomic Na $3p\ ^2P_{3/2}$ level is then made.

II. EXPERIMENTAL DETAILS

The experimental approach is a combination and refinement of hyperfine quantum beats and delayed-detection methods employed previously [3,10,11]. Generally, a well-collimated and polarized laser is tuned to atomic resonance, producing a distribution of atomic multipoles [12] in some level. The laser is presumed to be

much broader than the distribution of hyperfine components in the transition, and to have a temporal width W much smaller than any inverse hyperfine frequency in the excited level. The multipole distribution is probed at some later time T by a second broadband, short-pulse polarized laser tuned to a second atomic transition connecting the pumped level to some other suitable level. Measurement of an electronic polarization degree as a function of delay time T maps out beats in the polarization generated by the coherent electron-nucleus interactions. The pump and probe lasers are collinear and have readily characterized polarizations, implying a polarimeter of high analyzing power. In the experiments described here, the analyzing power was typically larger than 0.999. To obtain such high values in a resonance fluorescence experiment much of the signal would have to be discarded. A second advantage over a delayed-fluorescence approach is that a significant amount of the excited atoms remaining after the interval T contributes to the signal (the probe transition may be saturated with no reduction in the measured polarization). This is in contrast to delayed-fluorescence experiments, where only that portion of excited atoms remaining at time T and spontaneously radiating in the interval W contributes to the measured signal. These two advantages give an experimental approach having a high signal-to-noise ratio and negligible systematic errors associated with the polarization measurements.

As the quoted uncertainty in the hyperfine coupling constants is significantly smaller than other measurements, the following paragraphs contain a quite detailed description of our experimental approach and procedures. The atomic Na energy levels and transitions relevant to the basic pump-probe experimental scheme are shown in Fig. 1. A block diagram of the experimental apparatus in presented in Fig. 2. In the pump-probe approach illustrated there, the linearly polarized output from a short-pulse-dye laser (laser 1) excites the atomic Na $3p\ ^2P_{3/2}$ level, producing an electronic alignment in that level. The 590-nm laser output has a bandwidth of about 1 cm^{-1}, and an average pulse energy of approximately 10 μJ. A typical pulse width is ~ 0.5 ns. The electronic alignment [12] is probed by light from a second linearly polarized, short-pulse-dye laser (laser 2) tuned to the $3p\ ^2P_{3/2} \rightarrow 5s\ ^2S_{1/2}$ atomic Na transition at 616.0 nm. Laser 2 has spectral and temporal characteristics similar to those of laser 1. Excitation of the $5s\ ^2S_{1/2}$ level is

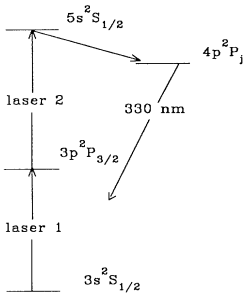

FIG. 1. Partial energy level scheme for atomic Na.

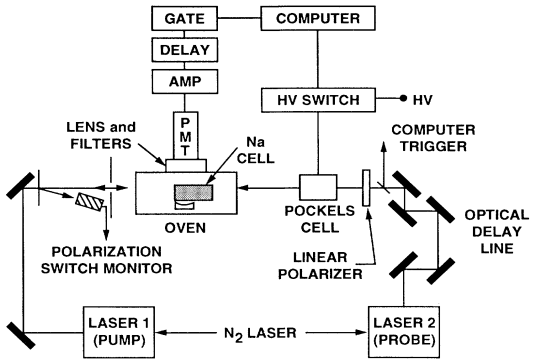

FIG. 2. Block diagram of the experimental apparatus. PMT denotes a photomultiplier tube and HV a high-voltage source.

monitored by detection of the intensity I of the $4p\ ^2P_j \rightarrow 3s\ ^2S_{1/2}$ cascade fluorescence at 330 nm. As shown in Fig. 2, measurement of the fluorescence intensity I is made in a direction perpendicular to the propagation directions of the pump and probe lasers, and perpendicular to the linear polarization direction of laser 1. This both reduces the amount of scattered laser radiation to be filtered and minimizes the effect of the temporal distribution of excited atoms viewed within the interaction region of the cell. The fluorescence is monitored by an EMI 9814 photomultiplier tube (PMT) mounted with interference and colored glass filters which eliminate scattered laser light and background radiation. A concave mirror is placed opposite the PMT in order to gather a larger portion of the fluorescence. The PMT is operated in a gated-photon counting mode, with the 500-ns gate opening typically 30 ns after the arrival of the probe pulse at the cell. The photon-counting signal is amplified, delayed, and used as the stop signal for a time-to-amplitude converter (TAC). The start pulse is provided by a triggering signal obtained from a photodiode which detects the delayed laser 2 probe pulse. The TAC signal is digitized and stored in a laboratory computer. A typical photon-counting rate of less than 0.1 per laser shot ensures that dead-time corrections to the data are small; corrections were made to the number of measured counts as required.

The dye lasers are excited by a short-pulse, 1-MW nitrogen laser which simultaneously pumps the pump (laser 1) and probe (laser 2) lasers. The lasers are pumped at a repetition rate of about 4 Hz. The dye lasers are of a grazing incidence type, where output coupling is from the zero-order reflection from the grating, and where a 100% high reflecting end mirror is used. Each laser beam is collimated to a width of about 2 mm. The output beam of each laser is passed through a high-quality linear polarizer, ensuring a linear polarization degree in each case of better than 0.999. The beam of laser 2 is then passed through a Pockels cell; application of the half-wave voltage to the Pockels cell changes the linear polarization direction of laser 2 from parallel to perpendicular to that of laser 1. With the half-wave voltage applied, the transmission of the probe laser beam through a linear po-

larization analyzer is reduced by about 10^{-4}. After passing the beam of laser 2 through two oven windows and the two cell windows, a slight birefringence generates a small amount of ellipticity in the probe beam (and in the pump beam as well). In either case, the total intensity of the "wrong" polarization component is less than 10^{-3} of the main polarization component. This produces an effect on the measured polarization entirely negligible compare to the size of the statistical uncertainty in the measurements.

The laser beams are passed through an oven containing a sealed and evacuated Na cell. The oven is heated to about 360 K by a coaxial heating element; the temperature was stable to typically 0.1 K. In order to minimize the effects of external, static magnetic fields on the results, the oven is situated in the center of two sets of Helmholtz coils. The cylindrical oven is also oriented so that its long axis is along the horizontal component of the Earth's field. With these arrangements, the mean static magnetic field in the central area of the cell was measured by a rotating-coil magnetometer to be less than 0.05 G. Cells within the oven are constructed from Pyrex tubing, are 6 cm long, and have a diameter of 2.5 cm; the cell windows are normal to the direction of propagation of the laser beams. Cells are processed by baking at 650 K under a vacuum of less than 10^{-6} Torr for 48 h. A small amount of Na metal is then distilled into the cells prior to sealing them off under vacuum. Under typical oven operating conditions, the Na vapor density in a cell is typically 10^{8} cm^{-3}.

Data acquisition, along with Pockels cell switching and monitoring, are computer controlled so as to ensure optimum performance of the polarimeter. Provision is made for selection of the total number of laser shots for each run and for the frequency of switching the laser 2 linear polarization direction. Typically, runs consist of 5000 laser shots, with the probe polarization being switched every five shots. This procedure minimizes systematic drifts in the polarization due to drifting in the average laser intensity and frequency. From the number of photon counts with a probe linearly polarized parallel ($I_{\parallel}$) or perpendicular ($I_{\perp}$) to the pump laser polarization direction, a polarization degree $P_L=(I_{\parallel}-I_{\perp})/(I_{\parallel}+I_{\perp})$ is formed. Dead-time corrected counts are used in all cases. Background counting rates were negligible. A time distribution of the accumulated photon counts is also obtained. This information is useful for diagnostic purposes. Proper application of a half-wave voltage to the Pockels cell is monitored by detecting, with a photodiode and linear polarizer combination, a small portion of the probe laser beam intensity after the beam exits the cell. The detector combination is such that correct application of a half-wave voltage reduces the normal $\sim$2 V signal to about 2 mV; the values are digitized and stored for each laser shot. This procedure allows for detection of small changes in the proper performance of the Pockels cell and its associated electronics. Rare switch failures and small drifts in the half-wave voltage are apparent.

The time delay T between the pump and probe lasers ranges from 4 to 135 ns, the maximum delay corresponding to more than 8 times the 16.3-ns radiative lifetime of the $3p\ ^2P_{3/2}$ level. A mechanical delay line in employed to generate the necessary long delays. The temporal delay between the two laser pulses is determined by directly measuring the path difference traversed by the laser beams, and converting this to a time delay through the speed of light in vacuum. The index of refraction of air under normal conditions has a negligible effect on this calculation of T. Small differential shifts due to propagation through refractive elements, beam splitters, the Pockels cell, and cell windows are accounted for by taking an index of refraction for these elements of 1.5. The length measurements are made by using a surveyor's steel tape measure. This measure is compared to two others made by different manufacturers; the three agreed to better than $\frac{1}{32}$ in. over a common 100 ft length. Sagging of the tape over the longest single path length (about 50 ft) adds a maximum of about $\frac{1}{8}$ in. to the measured length. This is fortuitously compensated to some degree in the usual measuring procedure by stretching of the tape by about the same amount. Thermal changes in the length of the tape are negligible. The overall uncertainty in the delay distance due to these effects is much less than 1 in., corresponding to a time delay of much less than 0.1 ns.

Calibration of the mechanical delay line is the most critical factor determining possible systematic error in the determined hyperfine beat frequencies. In the fitting procedure, what is determined at each delay time T is a set of products $\omega_{ff'}T$; a scale error in T produces a direct systematic error in the determined hyperfine frequencies. To check the calibration of the scale in a independent manner, a light-emitting-diode-based electronic range finder (TOPCON model GTS-303) was employed. This instrument determines distance by precisely measuring the phase difference, at several impressed modulation frequencies (147 kHz, 150 kHz, 30 MHz), between the diode source intensity and the intensity of the retroreflected beam. The mean standard error in measurement of a distance D is quoted to be $\pm(3\text{ mm}+2D/10^6)$. For a tape-measured interval of 89.23(1) ft, the electronic range finder gave a mean value of 89.254(2) ft. The difference of 0.024 ft corresponds to 0.29 in., or about 0.025 ns delay time. This difference is totally negligible on the scale of accuracy of our time measurements, and corresponds to the typical reproducibility of $\pm$0.25 in. in the distance measurements of the experiments.

The overall time delay was also directly confirmed (with lower accuracy) electronically in the experimental apparatus. This is accomplished by monitoring scattered laser radiation from the central region of the cell. The radiation is detected by the PMT in its usual location, but with the filters removed, and with two pin holes between the cell and the PMT. These optimize the time response of the PMT by minimizing the area of the photocathode illuminated. The PMT current is terminated into 50 Ω and the resulting voltage is directly monitored by a 400-MHz oscilloscope; the apparent laser pulse widths are about 1 ns under these conditions. To obtain the best measurement of the delay between the pulses, the PMT signal is split, with one-half being passed through a delay

line. That half is inverted and added to the other half. Minimizing the summed signal as a function of delay corresponds to a best measure of the time interval between the two pulses. A clear minimum could be detected with a resolution of about 0.1 ns. The delay line and associated amplifiers, inverters, and summer is then calibrated by replacing the PMT signal with one from a Hewlett-Packard 3336C radio frequency (0–60 MHz) synthesizer. The location of the various interference minima as a function of frequency permit calibration of the delay line to a precision of better than 0.01 ns. *Differences* between delay times measured mechanically and electronically agree to within their combined uncertainty of about ± 0.15 ns. As discussed in the results section of this paper, there exists an overall *shift* of $-0.22(7)$ ns between the two sets of local delay measurements. This is attributed to the somewhat different geometrical configurations of the pump and probe lasers. An overall shift of this size does not affect the values of hyperfine frequencies extracted from the data; only a calibration error in the scale can have an important effect on those frequencies.

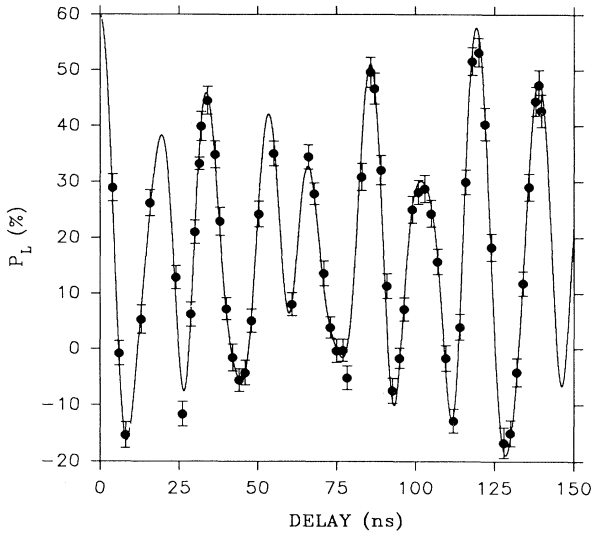

FIG. 3. Experimental data and best-fit curve showing the time evolution of the atomic Na $3p\,^2P_{3/2}$ level electronic polarization P_L.

III. RESULTS AND DISCUSSION

A linear polarization degree P_L is directly measured as a function of the delay time T between laser 1 and laser 2. The linear polarization degree is proportional to the electronic alignment in the $3p\,^2P_{3/2}$ level; the mean alignment [12,13] produced in the axially symmetric excitation process is defined as $\langle A_0\rangle = \langle \sum_m [3m^2/j(j+1)-1]\rangle$, where $\langle\ \rangle$ indicates an average over the magnetic substates of the excited level. For linearly polarized excitation, an initial alignment $\langle A_0(0)\rangle = -0.8$ is produced in the $3p\,^2P_{3/2}$ level. Because of the hyperfine interaction, the alignment evolves in time according to $\langle A_0(t)\rangle = \langle A_0(0)\rangle g(t)$, where $g(t)$ is a depolarization coefficient [12,14] given by

$$g(t) = \sum_f \sum_{f'} [(2f+1)(2f'+1)/(2i+1)]W^2(jfjf';i2) \times \cos(\omega_{ff'}t)\ .$$

Here $j=\frac{3}{2}$ is the electronic angular momentum, $i=\frac{3}{2}$ the nuclear spin, and f the total angular momentum quantum number. $W(\ )$ is a Racah coefficient and $\omega_{ff'}$ hyperfine frequency separations between the f and f' levels. The summations are over f and f'. In the absence of relaxation of the electronic or nuclear alignment by other processes, and in the absence of external fields, the time evolution of the electronic polarization [13] is given by $P_L = 3h\langle A_0(t)\rangle / [4 + h\langle A_0(t)\rangle]$. The parameter h depends on the initial and final angular momenta of the states involved in the probe transition; for the experiment here $h=-\frac{5}{4}$. Thus, fitting the measured linear polarization to this expression as a function of $t=T$ allows extraction of the implicit hyperfine frequencies $\omega_{ff'}$. These, in turn, are simply related to the magnetic dipole and electric-quadrupole coupling constants [1,4].

The delay time dependence of P_L is shown in Fig. 3, where the hyperfine quantum beats are evident. The polarization beats contain four frequencies $3A+B$, $5A$, $2A-B$, and $3A-2B$ parametrized in terms of the hyperfine coupling constants. Error bars on the polarization measurements were statistical, and determined from the photon-counting statistics. A sufficient number of runs at each delay were taken so that these were typically about $\pm 2\%$. The uncertainty in the delay time T due to uncertainty in the distance measurement (± 0.25 in.) is about ± 0.02 ns, and is negligible on the scale of Fig. 3. This estimate is made on the basis of the spread in repeated measurements of the delay distance by different experimenters.

The polarization measurements reported here are free of measurable systematic effects caused by pump or probe laser power, external magnetic field, Na density, and degradation due to unwanted background signal. Variations in the intensity of each laser by an order of magnitude produced no measurable change in the polarization. Similarly, there was no measurable background contribution to the signal due to PMT dark current or from any other source. The alignment will generally precess about the direction of a static magnetic field; a reduction in the measured electronic alignment was initially measured at longer delays. Compensation for the Earth's magnetic field in the manner described in the previous section eliminated the reduction. Application of an addition (about 1 G) to the Earth's field increased the size of this effect, confirming that Zeeman precession of the alignment was responsible for the effect. Final data runs were taken with external fields minimized. Finally, the measured polarization was also found to be reduced by an increase in the Na density. This is explained in terms of reabsorption of resonance radiation by atoms along the pump-probe laser axis. These atoms have a generally reduced electronic alignment compared to those prepared by laser excitation, and also have a different starting time for precession of that alignment in the nuclear field. Each of

these factors leads to a reduced polarization, should these atoms be detected during the probe phase of the measurement. This effect was minimized by doing the experiments at a low Na density of about 10^8 cm^{-3}, for which radiation trapping was found to be not detectable in any single set of polarization measurements. Inclusion of the possibility of very weak damping of the alignment in fitting the data did lead to a slight overall improvement in the fit. We hypothesize that the weak damping is due to residual radiation trapping in the data, an effect too small to be seen in a single data run.

In order to fit the data in Fig. 3, a four-parameter-weighted least-squares fit to P_L vs T was made. The parameters of the fit were A, B, and overall offset in the time base δ, and an assumed exponential damping constant λ for the polarization. Previous measurements, employing the same apparatus used in the experiment reported here [15], have shown that the temporal shape of the pump or probe laser output may be well characterized by a rectangular shape having a width $W=0.53(3)$ ns. Averaging the pump and probe times over such a pulse produces a frequency-dependent phase shift, for each oscillating component in the alignment, given by $2[\cos(\gamma_{ff'}W)-1)/(\gamma_{ff'}W)^2]$. The final fit to the 58 data points with four fitting parameters is shown as the solid curve in the figure. The quality of the fit is better seen in Fig. 4, where the residuals P_L(fit)$-P_L$(measured), normalized to the statistical error in each point, are presented as a function of T. The horizontal lines in the figure represent the mean residual of $-0.012(11)$, and the one standard error limits. The value of the mean residual is consistent with zero. The parameters and their associated standard deviations are given in Table I. It is important to note that the best-fit results for A and B are not sensitive to the size of the damping constant λ or to the width W. In fact, setting each of these quantities to zero

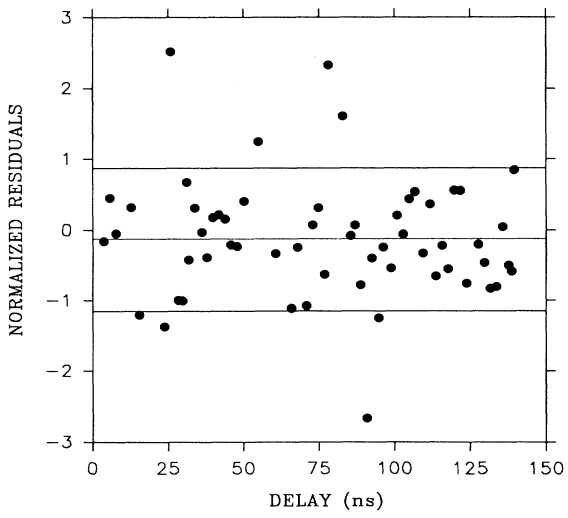

FIG. 4. Residuals of the fit shown in Fig. 3, normalized to the statistical uncertainty in each point. The horizontal lines represent the value of the mean residual and the one standard deviation limits. The mean residual of $-0.12(11)$ is consistent with zero.

TABLE I. Summary of the values of the fitted hyperfine coupling constants A and B, and the fitting parameters λ and δ.

A (MHz)	B (MHz)	λ (10^{-4} ns^{-1})	δ (ns)
18.534(15)	2.724(30)	3.7(1.1)	−0.22(7)

leads to no change in the final quoted digit of either A or B. Their inclusion does, however, reduce slightly the sum of the squared, weighted residuals of the fit.

Permitting the time zero δ to vary in the fit did have a significant effect (about two standard deviations) on the final values for A and B, even though the best-fit value for the shift was only $-0.22(7)$ ns. The shift very likely originates in the different physical characteristic of the pump and probe lasers, including a somewhat longer cavity length for the pump laser, and the different gain of the dyes used in the lasers. The path differences from which the delay time is determined is measured for each laser from a beam splitter which directs the ultraviolet nitrogen laser pump beam to the dye laser cells, and then along each laser beam path until the intersection point in the center of the Na sample cell. Thus the general characteristics of the lasers themselves are parametrized by the delay time δ as well as the pulse width W.

From the above discussion, the measured polarization and its time development are free from obvious systematic errors, either in the polarization measurements or in the determination of the time base. As discussed in this and in the previous section, the uncertainty in the time base due to length measurements is about ± 0.02 ns. Only an overall error in the calibration of the scale used to make the length measurements would increase this uncertainty. In fact, as such a scale miscalibration would increase in proportion to the distance measured, it would directly rescale the determined values of A and B in proportion to the miscalibration. As discussed in the previous section of this report, any such systematic effect is very small, and has a negligible effect on the measured values of A and B.

The many previous measurements of the Na $3p\ ^2P_{3/2}$ hyperfine coupling constants are presented in Table II. Also included is the recommended value from the compilation of Arimondo, Inguscio, and Violino [1]. Our result is in good agreement with that recommended value, being within one quoted error for B and within two quoted errors for A. A more recent measurement of the hyperfine structure by Krist *et al.* [9] is considerably more precise than any determination previous to the results reported here. This experiment employed the method of time-resolved hyperfine quantum beat spectroscopy. Our results for A and B are also in very good agreement with those or Kirst *et al.*, even though our measurement of the magnetic-dipole constant A is again lower by about two error intervals. The distribution of results from all measurements is more clearly seen in Fig. 5, which displays a scatter plot of A vs B. It is seen there that our result, indicated by a solid rectangle, is also within the general field defined by previous determinations. The dimensions of the rectangle indicate the uncertainty in A and B.

TABLE II. A summary of measurements of the hyperfine coupling constants A and B. The recommended values from Arimondo, Inguscio, and Violino (1977) are taken from Ref. [1].

A (MHz)	B (MHz)	Reference No.
18.534(15)	2.724(30)	This work
18.64(6)	2.77(6)	[9]
18.69(9)	2.90(21)	[1]
18.52(15)	2.98(34)	[16]
18.5(6)	2.25(40)	[17]
18.5(4)	3.0(6)	[18]
18.5(+6,−2)	3.2(5)	[19]
18.62(8)	3.04(19)	[20]
18.65(10)	2.82(30)	[21]
18.7(1)	3.0(2)	[22]
18.7(4)	3.4(4)	[23,24]
18.80(15)	2.9(3)	[25,26]
18.90(15)	2.40(15)	[27]
18.92(40)	2.4(4)	[28,29]
19.06(36)	2.58(30)	[30]
19.1(4)	2.5(4)	[31]
19.5(6)	2.4(14)	[32]
19.74(5)	3.34(4)	[33]

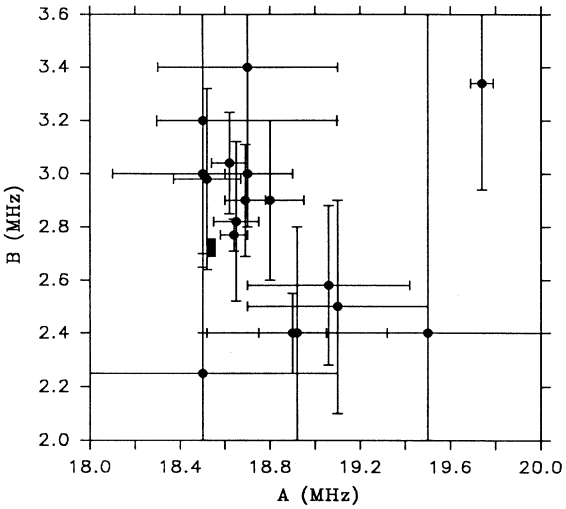

FIG. 5. A scatter plot of the A and B values listed in Table II. The result of this work is indicated by a rectangular solid area representing the uncertainty in A and B.

The results presented here for A and B have a precision more than a factor of 2 smaller than any other previous measurement of the Na $3p\,^2P_{3/2}$ hyperfine structure. The precision has been obtained by careful consideration of instrumental systematic errors associated with both the time base of the measurements and the analyzing power of the polarimeter. These factors have been discussed in detail in previous sections, and have been seen to contribute a negligible amount to the uncertainty in the hyperfine coupling constants. To ensure a reliable model for the analysis, systematic effects leading to destruction of the coherent precession of the nuclear and electronic angular momenta have been very nearly eliminated from the data set. The experimental method used also contributes significantly to the reliability of the results; after initial preparation of the system by the probe laser, it is allowed to evolve undisturbed for an extended period of time (relative to the natural decay time of the excited level). Thus the approach is nonperturbative and leads to a subnatural linewidth resolution in the experiment. Finally, at each delay time the polarization determination is normalized to a portion of the total signal intensity. Demands for a detector of large dynamic range and linearity are then much reduced from those experiments where the total intensity of the fluorescence is resolved in time.

Finally we comment on the impact of the present experimental results on the current reported discrepancy in the ^{23}Na nuclear-quadrupole moment as determined from atomic hyperfine measurements and as determined from muonic x-ray measurements. A recent paper by Sundholm and Olsen [7] has pointed out that the quadrupole moment Q as determined from hyperfine measurements is about 8% higher than the muonic value, with $Q_\mu = 100.6(20)$ mb and $Q_{\rm hf} = 108.9(32)$ mb. In the analysis, Sundholm and Olsen used the measured value for $B = 2.77(6)$ of Krist *et al.* [9] in extracting the quadrupole moment. Using instead our measurement of $B = 2.724(30)$ MHz leads to a revised value of $Q_{\rm hf} = 107.1(21)$ mb. The indicated uncertainty in this result is obtained by adding directly the statistical uncertainty in Q due to that in B to the quoted theoretical uncertainty in Q from Sundholm and Olsen. This more conservative method of combining the uncertainties from the measurements and the calculations is apparently the approach used by Sundholm and Olsen. A comparison of the previous result with the more precise one reported here reveals that $(Q_{\rm hf} - Q_\mu)/(\sigma_{\rm hf} + \sigma_\mu)$ is only about 1.6 in each case; $\sigma_{\rm hf}$ and σ_μ are the uncertainties indicated above. Thus, in spite of the significantly greater precision of the hyperfine coupling constants reported here, the conclusion of Sundholm and Olsen is not made stronger by our results.

ACKNOWLEDGMENTS

The contributions of David Olsgaard and Alex Beger to the research reported here is acknowledged. Financial support of the National Science Foundation (PHY-9121957) is greatly appreciated.

[1] E. Arimondo, M. Inguscio, and P. Violino, Rev. Mod. Phys. **49**, 31 (1977).

[2] A. A. Radzig and B. M. Smirnov, *Reference Data on Atoms, Molecules, and Ions* (Springer-Verlag, Berlin, 1985).

[3] W. Demtröder, *Laser Spectroscopy* (Springer-Verlag, Berlin, 1982).

[4] M. Weissbluth, *Atoms and Molecules* (Academic, New

York, 1978).
[5] C. E. Tanner, A. E. Livingston, R. J. Rafac, F. G. Serpa, K. W. Kukla, H. G. Berry, L. Young, and C. A. Kurtz, Phys. Rev. Lett. **69**, 2765 (1992).
[6] S. A. Blundell, W. R. Johnson, and J. Sapirstein, Phys. Rev. A **43**, 3407 (1991).
[7] D. Sundholm and J. Olsen, Phys. Rev. Lett. **68**, 927 (1992).
[8] W. Möller, H. Hühnermann, G. Alkazov, and V. Panteelev, Phys. Rev. Lett. **70**, 541 (1993).
[9] Th. Krist, P. Kuske, A. Gaupp, W. Wittmann, and H. J. Andrä, Phys. Lett. **61A**, 94 (1977).
[10] T. W. Ducas, M. G. Littman, and M. L. Zimmerman, Phys. Rev. Lett. **35**, 1752 (1975).
[11] P. L. Knight, Comments At. Mol. Phys. **10**, 241 (1981).
[12] K. Blum, *Density Matrix Theory and Applications* (Plenum, New York, 1981).
[13] C. H. Greene and R. N. Zare, Annu. Rev. Phys. Chem. **33**, 119 (1982).
[14] U. Fano and J. H. Macek, Rev. Mod. Phys. **45**, 553 (1973).
[15] L. Cook, D. Olsgaard, M. Havey, and A. Sieradzan, Phys. Rev. A **47**, 340 (1993).
[16] L. Windholz and M. Musso, Phys. Rev. A **39**, 2472 (1989).
[17] J. N. Dodd and R. W. N. Kinnear, Proc. Phys. Soc. London **75**, 51 (1960).
[18] G. Copley, B. P. Kibble, and G. W. Series, J. Phys. B **1**, 724 (1968).
[19] M. Baumann, W. Hartmann, H. Krüger, and A. Oed, Z. Phys. **194**, 270 (1966).
[20] H. Figger and H. Walther, Z. Phys. **267**, 1 (1974).
[21] D. Schönberner and D. Zimmermann, Z. Phys. **216**, 172 (1968).
[22] J. S. Deech, P. Hannaford, and G. W. Series, J. Phys. B **7**, 1131 (1974).
[23] H. Ackermann, Z. Phys. **194**, 253 (1966).
[24] H. Ackermann, in *La Structure Hyperfine Magnétique des Atomes et des Molecules,* edited by M. C. Moser and M. R. Lefebvre (CNRS, Paris, 1967).
[25] M. Baumann, Z. Naturforsch. A **23**, 620 (1968).
[26] M. Baumann, Z. Naturforsch. A **24**, 1049 (1968).
[27] R. W. Schmieder, A. Lurio, W. Happer, and A. Khadjavi, Phys. Rev. A **2**, 1216 (1970).
[28] S. Tudorache and I. M. Popescu, Stud. Cercet. Fiz. **23**, 1139 (1971).
[29] S. Tudorache, Stud. Cercet. Fiz. **26**, 361 (1974).
[30] M. L. Perl, I. I. Rabi, and B. Senitzky, Phys. Rev. **98**, 611 (1955).
[31] W. E. Baylis, Dr. Rer. Nat. thesis, Max-Planck Institut, München, 1967 (unpublished).
[32] P. L. Sagalyn, Phys. Rev. **94**, 885 (1954).
[33] A. L. Mashinskii, Opt. Spektrosk. **28**, 3 (1970).